Single-Shot Ultra-Fast Phase-Contrast X-ray Imaging of High-Pressure Diesel Fuel Sprays

Zunping Liu[1], Kyoung-Su Im[1], Xingbin Xie[2], Yujie Wang[1], Kamel Fezzaa[1], Ming-Chia Lai[2], and Jin Wang[1*]

[1]X-Ray Science Division, Argonne National Laboratory, 9700 South Cass Ave., Argonne, IL 60439-4800;
[2]Department of Mechanical Engineering, Wayne State University, 5050 Anthony Wayne Dr, Detroit, MI 48202.

Abstract

By taking advantage of high-intensity and high-brilliance x-ray beams available at the Advanced Photon Source (APS), ultrafast (150 ps) propagation-based phase-enhanced imaging was developed to visualize the high-pressure high-speed diesel spray breakup process in the optically dense near-nozzle region. The sub-ns temporal and μm spatial resolution allow us to capture the morphology of the high-speed fuel sprays traveling at >500 m/s with negligible motion blur. Both qualitative and quantitative information about the spray breakup can be readily obtained. In the experiment, two types of single-hole nozzles were used, a hydroground nozzle with rounded orifice inlet and a non-ground nozzle with a sharp inlet. The fuel sprays are extremely dynamic from both injectors. In the quasi-steady state of the injection, the jet from the hydroground nozzle (to a stagnant gas of 0.1 MPa) remains as a column showing two distinct instability regions showing surface instability waves and ligament-dominant breakup. The surface instability waves appear to be aerodynamics independent, while the downstream breakup is due to aerodynamic interaction between the jet and the ambient gas. Helium, nitrogen and sulfur hexafluoride at 0.1-MPa pressure are used as the ambient gases to test the aerodynamic interaction. In comparison, fuel injected from a nonground nozzle breaks up within several nozzle diameters from the nozzle exit. We speculate that internal-cavitation causes the jet to break up. For the hydroground nozzle, the surface waves exhibit as a new instability phenomenon at a condition with both high Weber and Reynolds numbers. These wave characteristics are extremely sensitive to the injection pressure, hence, the jet speed. The downstream aerodynamic breakup can be used to validate the theory proposed previously by Reitz.

Introduction

The breakup and atomization of fuel jets are the first and crucial steps for combustion. A detailed analysis of fuel sprays is known to be critical for understanding and optimizing the operation of internal-combustion engines. However, high-pressure injection of diesel sprays renders the near-nozzle region optically opaque mainly due to multiple scattering by the large number of droplets surrounding the jet. Visualization with conventional visible-light-based imaging techniques leads to no detailed information about the real structure and breakup of high-speed jets [1, 2]. Ultrafast x-radiography has revealed, for the first time, the fuel density distribution of this optically dense region [3, 4]. However, the true morphology of the sprays and the detailed breakup mechanism of the liquid fuel jets remains illusive because the x-radiograph contains only averaged spray density information. Third-generation synchrotron sources, such as the Advanced Photon Source (APS), produce x-ray beams with unique properties: extremely high intensity (10^{16} photon/s), wide tunability extending to a photon energy as high as 100 keV, high coherence, and flexible timing structure. These promise unique opportunities to allow the development of new and innovative x-ray-based visualization tools. X-ray phase-contrast imaging, with contrast from boundaries and interfaces of materials with different refraction index or abrupt thickness variations [5], has been demonstrated to visualize transient phenomenon dynamics [6]. More specifically, the contrast mechanism is based on diffraction and/or interference resulting from the differences in the real part of the index of refraction within the sample. Note that this is in addition to the normal absorption contrast mechanism. By using a phase-contrast mechanism, ultrafast imaging with a brilliant x-ray beam makes it possible to visualize high-pressure and high-speed diesel jets for the first time in the near-nozzle region, where most other techniques are not effective.

*Corresponding author, wangj@aps.anl.gov

Methods and Materials

Single-pulse phase-contrast imaging is possible at an ultrafast imaging setup at the XOR Sector 32ID beamline at the APS. As shown in Fig. 1, the x-ray beam is generated from an insertion device (undulator) in the APS electron storage ring. Ultrafast imaging requires a special filling pattern, a hybrid-singlet mode. This pattern contains a single electron bunch (150-ps duration and carrying 15 mA of current) and is separated from the rest of the electron bunches, which are in the form of 472 ns long, 94 mA by a 1.59 μs gap on both sides. The single bunch was used for this experiment. Most of the x-ray intensity was located within the first harmonic at 13.3 keV, with a peak irradiance of 10^{14} ph/s/mm^2/0.1% bw and a natural bandwidth of 0.3 keV full-width at half-maximum (FWHM). The x-ray beam was chopped by the millisecond and microsecond shutters at a rate of about 1 Hz, reducing the heating power of the beam by more than 99%. The spray images were formed on a fast scintillator crystal (LYSO:Ce) by converting the transmitted x-rays into visible light (432 nm) and were captured with a fast CCD camera (Sensicam HS-SVGA, 1024×1280 pixels, from Cooke) coupled with a microscope objective lens and a 45º mirror. The field of view of the imaging system is 680×855μm^2 or 1.3×1.7 mm^2 when a 10× or 5× objective lens (NA=0.14) is used, respectively.

The fuel spray was injected into a quiescent nitrogen gas ambient chamber using a common-rail injection system. A hydroground nozzle and a nonground nozzle were used. A gentle flow of the nitrogen gas (at atmospheric pressure and room temperature) was generated through a spray chamber in order to scavenge the fuel vapors.

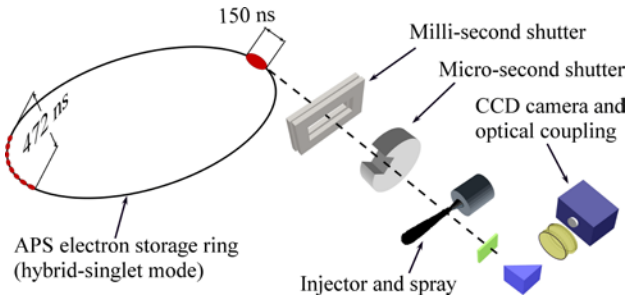

Figure 1. Schematic of the experimental setup.

Results and Discussion

At an injection pressure of 100 MPa and into a chamber filled with nitrogen gas of 0.1 MPa, the spray images were captured with both ultrafast x-ray phase-contrast imaging with 150-ps temporal resolution and visible-light shadowgraphy with 8-ns laser pulses. The sprays were injected from the hydroground and nonhydroground nozzles as shown in Fig. 2. As expected, the visible-light spray images (Figs. 2b and 2d) reveal no internal structural information about the sprays in the near-nozzle region mostly due to the high optical density. Therefore, our discussion on the sprays will focus on the images obtained by the x-ray method.

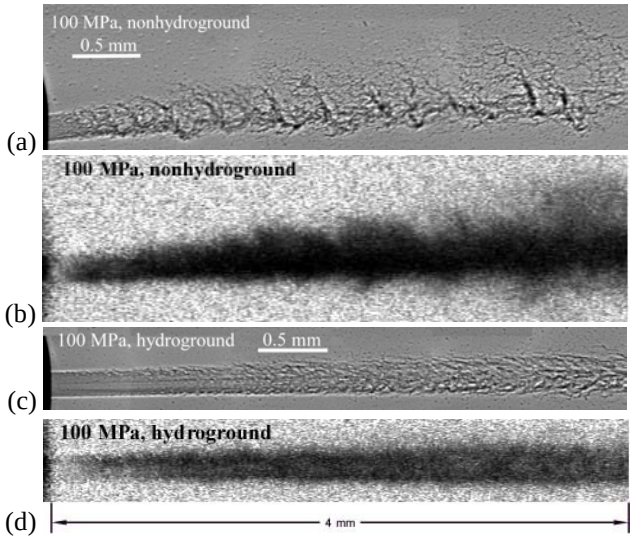

Figure 2. X-ray and visible-light spray images: (a) and (b) x-ray phase-contrast image and visible-light shadowgraph of the sprays from the nonground nozzle into stagnant nitrogen gas of 0.1 MPa at an injection pressure of 100 MPa, (c) and (d) x-ray phase-contrast image and visible-light shadowgraph of the sprays from hydroground nozzle injected under the same conditions.

Thanks to the image clarity afforded by the sub-ns exposure time and the phase-contrast mechanism, we can immediately observe the drastic difference in morphology between the sprays from the hydroground nozzle and the nonhydroground nozzle. The spray from nonhydroground nozzle (Fig. 2a) remains as a liquid column only within one diameter of the nozzle. Thereafter, it breaks up so that dispersed fuel ligaments and droplets are the main components of the spray. Most likely, the jet breakup is dominated by cavitation and so-induced pressure pulsations. The in-nozzle fluid dynamics simulation is underway to facilitating the understanding of those issues.

Sprays from different nozzle geometries:

In comparison, the spray from the hydroground nozzle exhibits a completely different structure in this near-nozzle region. In Fig. 2c, the jet remains as a liquid column within the first 2 mm from the nozzle exit. Upon close examination, one can observe a region with wavy structures. Beyond this point, ligaments have developed on the surface of the jet, presumably due to aerodynamic interaction between the jet and the ambient gas. The spray cone angle is much smaller in this case than that from the nonground nozzle (Fig. 2a). The visible-light shadowgraphs in Figs. 2b and 2d confirm the difference in the spray cone angles otherwise revealing no details of the jets.

Surface wave dependence of the injection pressure:

To better understand the sprays from the hydroground nozzle, we took x-ray images of the sprays injected at lower pressures (ranging from 45 to 100 MPa). Only the sprays injected at 50 and 70 MPa are shown in Fig. 3. At the lower pressure, the spray images show two distinct regions before the sprays fully break up: 1) a surface-wave region very near the orifice exit, and 2) a breakup region with ligaments at the jet surface.

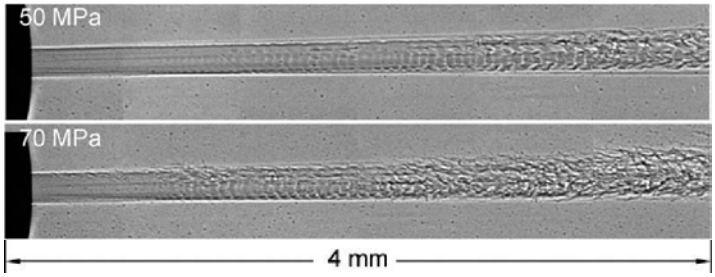

Figure 3. Single-shot ultrafast imaging of fuel sprays from a hydroground nozzle injected at 50 and 70 MPa into 0.1 MPa N_2 gas.

At a lower injection pressures, the wavelength of the near-nozzle surface waves is surprisingly monodispersed. The values of the wavelength are a fraction of the orifice diameter. With the pressure dependence of the spray structure, one can immediately observe the following qualitatively: the wavelength decreases upon an increase in the injection pressure. This pressure dependence is highlighted in Fig. 4, where the wave-length dependence on the injection pressure of the jet in both linear and log-log scales is plotted. The power-law dependence is immediately observed as the wavelength is inversely proportional to the injection pressure or the Weber number.

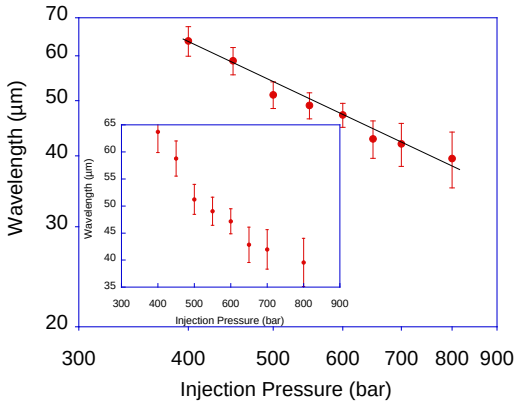

Figure 4. Injection pressure dependence of the wavelength of the surface waves near the nozzle exit.

Surface wave growth upon exiting from the orifice:

In Fig. 5a, we show the image of the spray when the injector is turned 90° around the spray axis. Comparing this image with that taken at 0° as shown in Figs. 2 and 3, the near-nozzle instability waves are indeed on the surface of the jet. With this viewing angle, one can directly measure the wave amplitude. The wave amplitude as a function of the distance to the nozzle exit is shown Fig. 5b at injection of 45, 47.5, 50, and 52.5 MPa. The normalized amplitude (A/D, by the nozzle diameter) of the wave can be best described as an exponential function of the normalized distance (x/D, by the nozzle diameter) to the nozzle exit,

$$A/D = A_0\left[e^{B(x/D)} - 1\right] \quad ,$$

where the growth rate, B, remains constant and has weak, if any, dependence on the injection pressure. This weak dependence indicates the grow rate is a constant for all injection pressures.

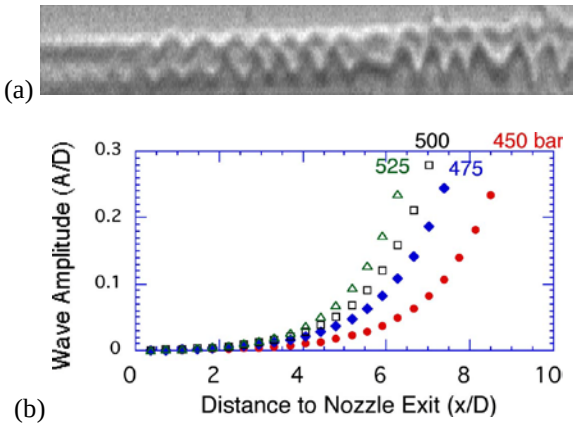

Figure 5. Wave growth: (a) x-ray image of the wave at the fuel jet surface, (b) the wave amplitude growth at lower injection pressures of 45, 47.5, 50, and 52.5 MPa.

Wave amplitude dependence on ambient gas density:

As a test on the origin of the surface waves in the nearest region of the nozzle exit, we used three types of gases in the study: He, N_2, and SF_6, all at 0.1 MPa at room temperature, corresponding to gas densities of 0.179, 1.25, 6.14 kg/m^3, respectively. If the surface instability waves are generated by aerodynamic interaction between the jet and the ambient gas, the wave amplitude should be biggest in the case where the jet was injected into the heaviest gas, SF_6. In fact, the wave amplitude is noticeably lower in SF_6 than in either He or N_2, as shown in Fig. 6. In Fig. 6a are shown the raw images of the surface waves in He, N_2 and SF_6. Figure 6b shows the comparison between the contrast (amplitude) values in all three cases. Here, we speculate that the initial surface instability does not have hydrodynamic origin, rather it could be from in-nozzle turbulence.

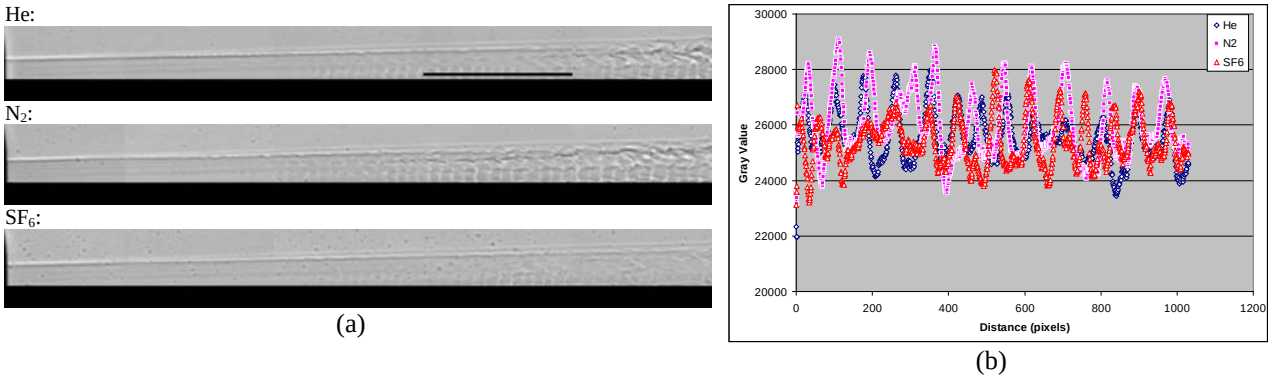

Figure 6. X-ray ultrafast imaging of the spray images in He, N_2, and SF_6, all at 0.1 MPa: (a) images and (b) comparison of typical line scans showing the contrast with SF_6 is the lowest in the three cases. The black line in the "He" image indicates the position for the typical line scans in all three cases.

Breakup ligament size depending on injection pressure:

In Fig. 7 we simply demonstrate that the average ligament size decreases as the injection pressure increases from 40 MPa to 100 MPa. The quantitative analysis is ongoing, and the results will be directly compared with Reitz's prediction of liquid jets [7] with high Weber numbers related to high-pressure conditions.

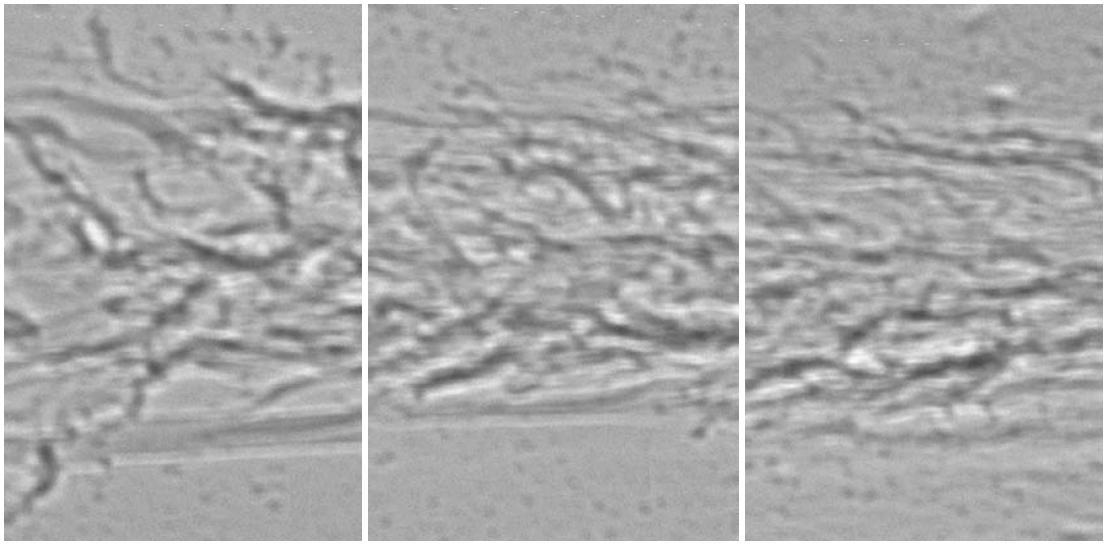

(a) (b) (c)

Figure 7. Images of spray sections for sprays injected at (a) 40, (b) 70, and (c) 100 MPa.

Conclusions

With the development of a 150-ps single-shot x-ray imaging capability, we discovered that high-pressure diesel sprays are sensitive to the details of the nozzle geometry. For a minimally disturbed jet, there are two distinct regions: the first region shows surface instability waves that are apparently not from aerodynamic interaction. Rather, aerodynamic interaction is responsible for the breakup through formation of surface ligaments.

Acknowledgement

This work at and use of the APS and CHESS are supported by U.S. Department of Energy, Office of Science, Office of Basic Energy Science, under Contract No. DE-AC02-06CH11357. The beamline support at the APS Sector 32ID is acknowledged. This work is also partially supported by the U.S. Department of Energy, Office of Vehicle Technology.

References

1. Smallwood, G. J.; Gülder, Ö. L. *Atomization and Sprays* 10:355-386 (2000).
2. Linne, M.; Paciaroni, M.; Hall, T.; Parker, T. *Experiments in Fluids* 40: 836-846 (2006).
3. **Yue, Y., Powell, C. F., Poola, R., Wang, J.,** and **Schaller, J. K.** *Atomization Sprays*, **11**, 471–490 (2001).
4. **Powell, C. F., Yue, Y., Poola, R.,** and **Wang, J.** *J. Synchrotron Radiat.*, **7**, 356–360 (2000).
5. Wilkins, S. W.; Gureyev, T. E.; Gao, D.; Pogany, A.; Stevenson, A. W. *Nature* 384:335-338 (1996).
6. Wang, Y.-J.; Liu, X.; Im, K.-S.; Lee, W.-K.; Wang, J.; Fezzaa, K.; Hung, D. L. S.; Winkelman, J. R. *Nature Physics* 4:305-309 (2008).
7. Reitz, R.D., *Atomization and Spray Technology* 3:309-337 (1987).